THE JOURNAL OF PHYSICAL CHEMISTRY C

Article

Study of Confinement and Catalysis Effects of the Reaction of Methylation of Benzene by Methanol in H-Beta and H-ZSM-5 Zeolites by Topological Analysis of Electron Density

Maria Fernanda Zalazar, Esteban Nadal Paredes, Gonzalo David Romero Ojeda, Néstor Damián Cabral, and Nelida Maria Peruchena

J. Phys. Chem. C, **Just Accepted Manuscript** • DOI: 10.1021/acs.jpcc.7b10297 • Publication Date (Web): 18 Jan 2018

"Study of Confinement and Catalysis Effects of the Reaction of Methylation of Benzene by Methanol in H-Beta and H-ZSM-5 Zeolites by Topological Analysis of Electron Density"

M. Fernanda Zalazar[1,2], Esteban N. Paredes[1], Gonzalo D. Romero Ojeda[1], Néstor Damián Cabral[1] and Nélida M. Peruchena[1,2]*

[1]Laboratorio de Estructura Molecular y Propiedades (LEMYP), Facultad de Ciencias Exactas, Naturales y Agrimensura, Universidad Nacional del Nordeste (UNNE), Avda. Libertad 5460, (3400) Corrientes, Argentina.

[2] Instituto de Química Básica y Aplicada del Nordeste Argentino, IQUIBA-NEA, UNNE-CONICET, Avenida Libertad 5460, (3400) Corrientes, Argentina.

* Corresponding authors.

Email address: mfzalazar@conicet.gov.ar (M .F. Zalazar)

Keywords: Heterogeneous Catalysis, Carbenium ions, host-guest interactions, DFT, Quantum Theory of Atoms in Molecules (QTAIM)

ABSTRACT

In this work we studied the host-guest interactions between confined molecules and zeolites, and their relationship with the energies involved in the reaction of methylation of benzene by methanol in H-ZSM-5 and H-Beta zeolites employing DFT methods and the Quantum Theory of Atoms in Molecules. Results show that the strength of the interactions related to adsorption and co-adsorption processes are higher in the catalyst with larger cavity; however, the confinement effects are higher in the smaller zeolite, explaining from an electronic viewpoint the reason why the stabilization energy is higher in H-ZSM-5 than in H-Beta. The confinement effects of the catalyst on the confined species for methanol adsorption, benzene co-adsorption and the formed intermediates dominate this stabilization. For the transition state, the stability of the TS is achieved due to the stabilizing effect of the surrounding zeolite framework on the formed carbocationic species (CH_3^+) which is higher in H-ZSM-5 than in H-Beta. In both TS the methyl cation is multi-coordinated forming the following $H_2O\cdots CH_3^+\cdots C_B$ concerted bonds. It is demonstrated that through the electron density analysis it can be defined the criteria to discriminate between interactions related to the confinement effects and the reaction itself (adsorption, co-adsorption, bond breaking and bond forming processes) and thus to discriminate the relative contributions of the degree of confinement to the reaction energies for two zeolite catalysts with different topologies.

1. Introduction

Zeolites are microporous/nanoporous solids widely used in fine chemicals and petrochemicals as heterogeneous catalysts. They possess pores, cavities and channels with well-defined molecular dimensions.[1] These three-dimensional cavities provide a selective environment, in which a chemical reaction occurs. The confinement effect was proposed to explain the interactions between the zeolite framework and the adsorbed molecules. It plays an important role on adsorption and catalytic properties of zeolites by stabilizing adsorbed molecules, intermediates, and transition states. Due to the confinement effects, zeolites can be described as solid solvents.[2]

Confinement and solvation by van der Waals forces confer remarkable diversity to zeolites, in spite of their structural rigidity and their common aluminosilicate composition.[3] Gounder and Iglesia discussed how electrostatic interactions and dispersion forces depend on the structure of the zeolitic cavity, its composition, and how confined transition states and intermediates are stabilized, and how these interactions influence elementary steps in a catalytic cycle.[3] However, the authors concluded that a more rigorous assessment of the consequences of solvation effects in catalysis and their distinction from weaker effects of acid strength is necessary. Additionally, only a small fraction of the large number of currently available zeolites is used in practice, reflecting an incomplete knowledge of how such structures influence reactivity by solvating intermediates and activated complexes.[4]

The confinement effects on zeolites have received much attention over the last years and several studies on the role of confinement have been conducted by using several methodologies. Among previous research, Gounder and Iglesia studied the confinement effect on the selectivity of alkane cracking and dehydrogenation in MOR, MFI, FER and USY zeolite pockets.[5] Li *et al.*[6] studied the dimensional match between zeolite cavities and organic species involved in hydrocarbon pool mechanism. Using geometrical parameters and energies at ONIOM (B3LYP/6-1G(d,p):AM1) level they pointed out that the differences in reaction barriers and reaction energies are highly related to the different confinement effects of zeolite cavities. They studied the interactions related to confinement comparing different zeolite cavities, taking into account the closest contacts between hydrogen atoms of guest molecules and oxygen atoms of catalyst ($O_{zeolite}\cdots H_{guest\_molecule}$

distances < 3.0 Å) and related them with energy barriers of the reaction. The CHA zeolite cavity matches the dimensions of hydrocarbon pool species better than LEV and LTA zeolites, so it is able to provide the most suitable confinement to organic species.[6]

Likewise, Mazar *et al.* ascertained the degree of confinement, or "local" dispersion energy (E_{LDE}), experienced by species confined inside zeolite cages following a counting procedure where they considered distances ranging from r_{min} (1.9 Å) to r_{max} (5.1 Å) between the atoms of guest molecule and the catalyst.[7] The lower limit (r_{min}) was chosen so that it exceeded all covalent bond lengths while the high value (r_{max}) ensured the counting of all interatomic distances between the species of interest and the zeolite pore wall in the most confined case. Then, they identified the number of van der Waals interactions and calculated the E_{LDE} of the species of interest by applying the appropriate van der Waals coefficients.[7]

De Moor and co-workers studied adsorption of alkanes in zeolites and showed that smaller pores lead to a tighter fit of adsorbates and thus to stronger adsorption, mainly due to higher contributions of the stabilizing van der Waals interactions between the n-alkane and the zeolite.[8] According to Sacchetto and co-workers, the knowledge of host−guest interactions occurring in zeolites could be helpful to improve adsorption properties of these materials, thus extending their application fields.[9] Using FTIR and SS-NMR spectroscopy and computational calculations they showed that interactions between pollutant molecules and zeolite cavities play a key role in the adsorption process.

Recently, Resasco and co-workers revised the importance of confinement effects on activity and stability of small oxygenates compounds in the chemistry of coupling reactions for biomass conversion on zeolites[10] and suggested that the combination of acid strength and dispersive forces and confinement near the Brønsted acid site (BAS) is responsible for the great diversity of reactivity and selectivity displayed by different zeolites. Moreover, Sastre reviewed the relative stability of different intermediates involved in the process of methanol-to-olefins in terms of confinement effects in different cage-based zeolites.[11] Other authors in order to discriminate the confinement effect compared the energy barriers between small and larger zeolite models calculated at the same level or compared calculations using functionals with and without dispersion terms, and significant differences were found when confinement is taken into account.[12]

The previous works cited have reported the study of the confinement effect by using different experimental and theoretical methodologies. However, none of them have addressed the study of this effect from the viewpoint of analysis of electron charge density distribution in order to provide new insights to increase our understanding of the confinement effects by solid acid catalysts.

Our previous studies using small zeolite cluster models have exposed the relevance of the information that can be obtained through the topological analysis of electron density and its Laplacian on the study of chemical reactions of interest in the zeolite chemistry. For example, in a previous work we showed that the most important topological feature in the ethene protonation reaction over acidic zeolite is the electron charge density redistribution.[13] Additionally, we also studied the electron density redistribution, not only on the stationary points of these chemical reactions, but also along the intrinsic reaction coordinate (IRC) connecting the stationary points and we identified the different regions of these chemical reaction in terms of the charge redistribution process.[14] In other work, we used the topological analysis of the Laplacian of electron density distribution as a tool to investigate the stereoelectronic control of chemical reactions.[15] These previous studies showed that the stabilization and formation of intermediates and transition states, depend on the availability of electrons in the zeolite framework. Therefore, electronic availability plays a key role to stabilize the formed species.

Furthermore, from electron density analysis on adsorbed alkenes on acidic zeolite model we showed that adsorption energy can be partitioned into two contributions: the primary and the secondary contribution.[16] The primary and also the principal contribution involved few atoms at the zeolite bifunctional acid site (defined as O–H···π interaction and other C–H···O interactions), and the secondary contribution (due to the environment). Because the small 5T zeolite cluster model used, only the primary contribution was considered, and thus the confinement effects were not calculated. Even so, we showed that we can discriminate specific interactions related to the active site of catalyst from the others interactions.

In the present work we study the adsorbate-catalyst interactions between confined molecules and zeolites, and their relationship with energies involved in the reaction. The Quantum Theory of Atoms in Molecules (QTAIM)[17-19] is applied in order to gain a deeper

understanding of electronic features that take place in the cavity of the catalyst and its role in the effect of confinement. We selected the reaction of methylation of benzene by methanol in H-ZSM-5 and H-Beta zeolites as a case study. The main purpose of this work is to provide an answer to the following questions: (a) Which interactions are established between the zeolite and the guest molecules? (b) What is the nature of these bonding interactions? (c) What is the influence of lattice atoms on stabilizing the adsorbed/co-adsorbed molecules, transition states and intermediates when different zeolites are considered? (d) Can the confinement effect be discriminated from the reaction itself and rationalized in terms of its relative contribution to the total process? Methylation reactions catalyzed by acidic zeolites are very important in several transformation processes of hydrocarbons, as conversion of methanol-to-gasoline (MTG) and methanol-to-olefins (MTO) processes.[20] Therefore, our results may provide a further insight into the confinement effect of zeolite cavities during the MTO conversion.

2. Method and Calculation Details

In the present work we study the host-guest interactions between catalyst and confined molecules and their relationship with energies involved in the reaction. We selected the reaction of methylation of benzene by methanol in H-ZSM-5 and H-beta zeolites as a case of study. To cover the confinement effect from the zeolite framework, the zeolite catalyst has been modeled by a 46T (T = Si and Al tetrahedral sites) for H-ZSM-5 and 52T for H-Beta quantum cluster model, with an overall composition $[O_{3/2}SiH]_{24}[OSiH_2]_{12}[SiO_2]_8[O_{3/2}Si(OH)AlO_{3/2}]$ and $[O_{3/2}SiH]_{34}[OSiH_2]_{14}[SiO_2]_2[O_{3/2}Si(OH)AlO_{3/2}]$, respectively.

These extended cluster include the cavity that emerged at the channels intersection of the catalyst and, therefore local effects (interaction of adsorbates with the Brønsted and Lewis sites) and nonlocal effects (van der Waals interactions with the zeolite cavity or confinement effects) are taken into account. The active site was positioned at the intersection channel because these locations offer maximal available space, result in minimal restrictions and has been chosen as the active site for the study of several reactions.[20-23] We have employed similar cluster model in our previous works on the adsorption of acetic acid and methanol on H-Beta.[24]

The geometries of all species were optimized without any constraint, except for the terminal H atoms of the zeolite that were held fixed during geometry optimization. The M06-2X[25-26] density functional and the 6-31G(d,p) basis set were used in all calculations, energy calculations using the B3LYP functional were also included for comparison. In order to obtain more accurate interaction energies, single point calculations with the 6-31++G(d,p) basis set were carried out. Previous studies showed that the density functional theory using the M06-2X functional provided quite good results compared to functionals without dispersion energy terms for study the interaction of organic molecules inside the zeolite pores [24, 26-31].

All stationary points were characterized by calculating the Hessian matrix and analyzing the vibrational normal modes. From each optimized geometry, vibrational modes were used to obtain zero-point vibrational energies and finite temperature corrections required to calculate enthalpies. All calculations were performed with the Gaussian 09 program.[32]

The topological analysis of the electron charge density distribution in the framework of atoms in molecules theory (AIM)[17-19] has been carried out for the present study. Total electron densities were obtained at M06-2X level using a 6-31++G(d,p) basis set, and the Gaussian program. The bond and atomic properties were calculated using the AIMAll software[33]. The maps of molecular electrostatic potential (MEP) of the isolated zeolites were calculated and drawn with AIMAll program using a 0.001 a.u. electron density isosurface.

The Bader´s net atomic charges were determined on selected atoms. The accuracy of the integration over the atomic basin (Ω) was assessed by the magnitude of a function $L(\Omega)$, which in all cases is less than 10^{-5} au. for H atoms and 10^{-4} au. for other atoms. We have employed similar QTAIM analysis in our previous works on the reaction of alkenes over acidic zeolite. [13-14, 16]

3. Results and Discussion

As far as the mechanism of the zeolite-catalyzed methylation reaction is concerned, two different proposals have been advocated in literature: a stepwise route that involves a surface-bound methoxy group intermediate, and a concerted mechanism in which

physisorbed methanol directly interacts with the species to be methylated.[20, 34-35] In this work only the concerted mechanism is considered, since experimental kinetic measurements are explained by this mechanism.[35-36] The confinement effect of different zeolite cavities (H-ZSM-5 and H-BETA) are evaluated assuming the same mechanism.

Figure 1 displays the most stable structures for concerted mechanisms and labels the stationary points described in the following discussion. Their corresponding energies are collected in Table 1. The transition states explored are carbenium ion-like. Next, we discuss the peculiarities of concerted mechanism briefly.

<Figure 1>

In the concerted mechanism, MeOH reacts directly with the hydrocarbon in a single step to form a methylated product and H_2O, thus, protonation and C-C bond formation occur simultaneously in one step, and an intermediate is not required as the reaction proceeds via coupling of adsorbed methanol on BAS with the species that is being methylated.[35] The initial step starts with the physisorption of a methanol molecule on the Brønsted acid site (BAS) of the zeolite (Fig. 1-**a**). Subsequently, a second benzene molecule is weakly co-adsorbed onto the first one (Fig. 1-**b**). The next step along the reaction coordinate is the transition state that describes the formation of the new C−C bond (TS). At the TS, the acidic proton of the zeolite (H_Z) has protonated the methanol molecule, and the C_M−O_M bond of methanol is cleaved leading to the formation of a methyl cation (CH_3^+) and a water molecule. Simultaneously, the positive charge that appears on the carbon atom (C_M) of methyl cation interacts with a carbon atom (C_B) of the π-cloud of the benzene, while the new C_M-C_B bond between the methanol and benzene molecules forms. Transition state involves a carbenium ion where the attacking methyl cation is almost planar. The transition states are very similar in both catalysts in accordance with other authors.[20] Then, the formation of the bond between C_M and C_B gives rise to a methylbenzenium ion (intermediate, Fig. 1-**d**) and a water molecule confined in the zeolite. The intermediate ion could deprotonate rapidly, regenerating the BAS of the zeolite.

Our energy results display similar values than those reported by other authors with similar methodologies.[20] The calculated energy for methanol adsorption in H-ZSM-5 is close to the experimental value reported as -27.5 kcal mol^{-1} at 400 K,[37] no experimental data for methanol adsorption on H-Beta are found in the literature. As we have mentioned

earlier, our previous results suggested that the energetic factors are not the only ones to be taken into account, when a chemical reaction is studied.[13, 15] In this case, the confinement effect is of paramount importance (which, in turn, depends on the specific structure of each zeolite) and beyond the energetic factors, it is important to consider the role of the weak host-guest interactions and their contribution to the total energy involved in the reaction.

The gas phase reaction versus the adsorption and confinement effects on the reaction inside the zeolite cavities could be compared. However, a previous study by Arstad *et al.* concluded that gas-phase schemes (where the acidic zeolite is represented as only one proton H^+) showed large relative energy differences between neutral and cationic species.[38] Furthermore, it should be emphasized that species obtained in the potential energy surface on gas phase reaction will be different from those found inside zeolites, where the movement of the guest molecules is restricted due to the influence of both zeolite pore size and shape selectivity. Thus, we propose that these effects can be evaluated through the analysis of the electron density distribution.

Molecular Electrostatic Potential

The use of topological analysis based on electron density distribution and, in conjunction with MEP maps provide valuable information about the steric volume, shape, and electronic properties of zeolite framework. The electrostatic potential is accordingly an effective means of predicting close contacts and noncovalent interactions, where in general, regions of positive electrostatic potential tend to interact favorably (at least initially) with negative sites and regions of negative electrostatic potential with positive sites.[39] MEPs are well suited for analyzing processes based on the "recognition" of one molecule by another, as in drug–receptor and enzyme–substrate interaction, because it is through their potentials that the two species first "see" each other.[40] In the same way one could thus argue, that MEPs could be of particular interest to predict adsorbate-catalyst interaction mode.

Figure 2 shows tri-dimensional molecular electrostatic potential maps at the van der Waals surface, representing electrostatic potentials superimposed onto a surface of constant electron charge density (0.001 e/au.^{3}). The electrostatic potential provides a representative measurement of the overall molecular charge distribution. The value of the electrostatic potential ranges from – 32.81 kcal mol^{-1} (deepest red) to + 61.80 kcal mol^{-1} (deepest blue).

From the figure it is clear that the most negative regions (red regions) are localized over the oxygen atoms inside the cavity of the catalyst where electron density is concentrated, and the most positive region (blue region) is localized over the BAS of zeolite where there is low electron density. The high electron density available inside the cavity shows the high availability of sites for interaction with electron deficient sites in guest molecules. Thus, it is of particular importance to quantify the confinement effect in terms of electron density distribution.

<Figure 2>

Electron density topology

The topological analysis of electron density, $\rho(r)$, and its Laplacian function, $\nabla^2\rho(r)$, constitutes a powerful tool to investigate the nature of the chemical bonds.[17] According to the Bader theory, the presence of a bond path (BP) is a universal indicator of the existence of a bonding interaction.[41]

The molecular graphs of electron density for the most stable structures in both zeolites are shown in Figures 3 and 4. From topological electron density calculations, a large quantity of bond, ring and cage critical points (CPs) appears. However, only the most meaningful bond critical points (BCP) with respect to the reaction and confinement phenomena are analyzed and discussed in detail. The topological analysis of these species shows the presence of several interactions among organic molecules, as well as among the organic molecules and the oxygen atoms of the zeolitic fragment. The BCP and the linking bond paths detected among the atoms involved in the reaction site for the three species are highlighted. In Tables 2-5, the bond distances and the most relevant topological properties of the electron density at the BCP for most stable structures are shown: the electron densities [$\rho(r)$], the Laplacian of the electron density [$\nabla^2\rho(r)$], and the total energy density, [$H(r)$].

<Figure 3>

<Figure 4>

The local topological properties at the BCP can be used to describe the strength of a bond. In general, the larger the magnitudes of $\rho(r)$, $\nabla^2\rho(r)$ and $H(r)$, the stronger the bond.[17] Additionally, the sign of the total energy density, defined as the sum of the potential and

kinetic energy densities at a critical point is an indicator of covalence in chemical interactions.[42-44] Thus, negative $H(r)$ values indicate a significant sharing of electrons.

Adsorbed methanol

Methanol adsorption inside zeolites is a research topic on which several studies, both experimental and theoretical, have been reported in the literature.[24, 45-53] In the papers mentioned above attention was mainly focused on the interaction between the methanol and the zeolite acid site. The presence of two hydrogen bonds have been described: the first being medium to strong and the second being much weaker. Even though these are the main adsorbate-catalyst interactions, due to the nature of the catalyst and the presence of several oxygen atoms therein (and large electron density inside the cavity, Fig. 2), we postulate that there should be several more framework-guest interactions and thus their relationship with adsorption energy should be significant.

Accordingly, for the QTAIM analysis we partitioned the adsorbate-catalyst system in two subsystems: the first one is related to the reaction itself and involves the interactions between the adsorbate and the active site of the zeolite [the proton of BAS (H_Z) and the oxygen (O_{Z2}) of the Al-O-Si bridge]; the second involves interactions between the organic molecule and the rest of the oxygen atoms of the catalyst (O_Z).

As it was expected, the topological analysis based on the electron density shows in both catalysts the presence of two principal interactions O_{Z1}-$H_Z\cdots O_M$ and O_M-$H\cdots O_{Z2}$ between the confined methanol and the active site of the zeolite. In addition, several weak interactions with the zeolite walls [denoted as C_M-$H\cdots O_Z$ and O_M-$H\cdots O_Z$] are observed, we related the latter to the confinement effects (see Figures 3a and 4a). The nature of these interactions can be evaluated through the electron density properties at the BCP (Table 2).

The topological properties at the BCP in the two main interactions: O_{Z1}-$H_Z\cdots O_M$ [between the proton of hydroxyl group of Brønsted acid site (H_z) and the oxygen atom of methanol (O_M)]; and O_M-$H\cdots O_{Z2}$ [between the hydrogen atom of hydroxyl group of methanol and the O_{Z2}] indicate that these ones are hydrogen bond interactions, HB. However, it is interesting to point out that in H-Beta both interactions are stronger than in H-ZSM-5. The O_{Z1}-$H_Z\cdots O_M$ interactions in H-Beta can be considered to be hydrogen bonds with very strong strength according to their topological properties (For strong H-

bonds, $\nabla^2\rho$(r) is positive and H(r) is negative, for very strong H-bonds, $\nabla^2\rho$(r) is negative and H(r) is negative).[54] The main interaction related with the adsorption process on the zeolite acid site (O_{Z1}-$H_Z\cdots O_M$) represents 75 % of total density contribution in H-ZSM-5 and 80.5 % in H-Beta.

Concerning the confinement effects, three C_M-H$\cdots O_Z$ interactions (between the hydrogen of methyl group of methanol and oxygen atoms of the framework) are found in H-ZSM-5 and four in H-BETA. These interactions show large bond distances ($d_{X\cdots Y}$ > 2.9 Å) and topological characteristics of very weak closed-shell interactions [ρ(r) < 0.01 u.a.; $\nabla^2\rho$(r) > 0 and H(r) > 0]. However the presence of several interactions contributes to the stabilization of adsorbed methanol. Additionally, the O_M-H$\cdots O_Z$ interaction (where the hydroxyl group of methanol interacts with another oxygen atom of the zeolite) shows larger ρ(r) values, $\nabla^2\rho$(r) > 0 and H(r) > 0, being typical values of closed-shell interactions, with large bond distances. The contribution of these weak interactions to the confinement effect is higher in H-ZSM-5 (representing 13.7 % of the total density) than in H-Beta (12.2 %), giving an idea of the effect of the size of the cavity in relation to the confinement effect and the adsorption energy. This is reflected in a greater stabilization of confined species within the cavity of H-ZSM-5.

Co-adsorbed benzene onto methanol complex

The next step involves the co-adsorption of benzene onto methanol complex. In this case, the topological analysis shows in both catalysts the presence of one principal interaction between the confined methanol with the acid site (O_{Z1}-$H_Z\cdots O_M$) and another interaction between the two confined species (methanol and benzene or guest-guest interactions). We related the latter to the co-adsorption of benzene onto adsorbed methanol (denoted as C_M-H$\cdots C_B$).

The O_{Z1}-$H_Z\cdots O_M$ distances are shorter than in methanol adsorption (1.16 vs 1.36 Å in H-ZSM-5 and 1.14 vs 1.27 Å in H-Beta) and the interaction is stronger, as it would be expected (Table 3). In this case ρ(r) is high, $\nabla^2\rho$(r) < 0 and H(r) < 0 shows characteristic of shared interaction. The last one suggests that benzene is co-adsorbed on protonated methanol, which indicates that the $H_Z\cdots O_M$-H_M bond of water molecule is already close to being formed at this co-adsorption step.

It is interesting to note that the benzene molecule is co-adsorbed by an interaction C_M-H$\cdots C_B$ type in H-ZSM-5 and, by two interactions C_M-H$\cdots C_B$ and O_M–H$\cdots C_B$ in H-Beta. The C_M-H$\cdots C_B$ distances are shorter in H-ZSM-5 than in H-Beta by 0.1 Å, and in both complexes the interaction shows characteristic of weak interaction. H(r) values are positive, which suggests poor electron sharing between guest-guest molecules.

In addition, several weak interactions with the zeolite framework are observed, we related these last ones to the confinement effects. We can clearly identify four different types of interactions: 11 C_B-H$\cdots O_Z$ interactions in H-ZSM-5 and 8 in H-Beta; 5 $O_Z\cdots\pi$CC in H-ZSM-5 and 4 in H-Beta; 4 C_M-H$\cdots O_Z$ in H-ZSM-5 and 2 in H-Beta; finally one O_M-H$\cdots O_Z$ interaction in H-ZSM-5 (See Figures 3b and 4b). All these interactions show $d_{X\cdots Y}$ > 2.4 Å. In both adsorbed complexes the C_B-H$\cdots O_Z$, $O_Z\cdots\pi$CC and C_M-H$\cdots O_Z$ BCP show relatively low values of ρ(r), positive values for $\nabla^2\rho$(r) and H(r) > 0, showing characteristics of closed shell interactions. It is interesting to highlight that in $O_Z\cdots\pi$(CC) a bond critical point between the O zeolite atom and the middle point of a CC bond of the benzene molecule can be found.

We observe again that the contributions of weak interactions to the confinement effect are higher in H-ZSM-5 than in H-Beta (representing 38.9 % of total density in H-ZSM-5 and 26.3 % in H-Beta). In addition, the stabilization energy is larger in H-ZSM-5 than in H-Beta indicating that the interactions related to the confinement effects are of great importance in the stabilization of the guest molecules in the zeolite pores, as shown by the molecular graphs.

Van der Mynsbrugge and co-workers found that benzene co-adsorption energy is larger in H-ZSM-5 (-25.3 kcal mol^{-1} at B3LYP-D3 level) than H-Beta (-21.98 kcal mol^{-1}), and it is attributed to a tighter fit of the guest molecules in the H-ZSM-5 zeolite pores or more empty space at the active site of H-Beta.[20] However, we suggest that this effect is not only due to the better fit of the reactant molecule on the zeolite cavity. The analysis derived from topological properties of the electron density distribution allows associating each interaction with a particular phenomenon of the process, discriminating adsorption from co-adsorption and from confinement, as well as confinement of benzene from confinement of methanol. In other words, these interactions can be rationalized in terms of their relative contribution to the total process. Thus, in co-adsorbed complexes, the relative process of

the methanol adsorption represents 58.3 % of total electron density contribution in H-ZSM-5 vs 65.5% in H-Beta, the co-adsorption of benzene 2.8 % in H-ZSM-5 vs 8.1 % in H-Beta and the confinement 38.9 % in H-ZSM-5 vs 26.3 % in H-Beta.

This analysis leads to the following conclusion: the strength of the interactions related to adsorption and co-adsorption process is higher in the catalyst with larger cavity; however, the confinement effects in the smaller zeolite are higher. From an electronic viewpoint this explains why the stabilization energy is higher in H-ZSM-5 than H-Beta, and that stabilization is dominated by the confinement effect of the catalyst on the reactant species.

Transition states

In the TS, the key interactions are O_M–H_Z bond formed (between methanol and the acidic proton of the zeolite); $C_M \cdots O_M$ bond breaking (in methanol) and $C_M \cdots C_B$ bond forming (between the methyl carbocation and benzene), being the latter responsible for the new C-C bond in the product (Table 4).

In both zeolites the size of guest molecules is the same for each step of the reaction (See Fig. S2 of supporting information). It can be seen that the stabilization energies are greater for adsorbed and co-adsorbed species, as well as for the intermediate in the zeolite of small cavity. Additionally in both catalysts, the properties of interactions related to bond forming and bond breaking are similar in TS. Nevertheless, differences are observed when comparing the magnitudes of the activation energies, where energies are higher for the small zeolite. It is interesting to highlight that energy stabilization by the framework is particularly important in the transition state. The TS formation involves a rearrangement of the electron densities of the π-cloud of benzene in order to be aligned on the methyl carbocation, as we showed in our previous work.[15]

At the TS the carbon atom of methyl cation (C_M) is bonded to five atoms, one carbon atom of benzene, an oxygen atom of formed water, and three hydrogen atoms. The most interesting features are the relatively short $C_M \cdots C_B$ and $C_M \cdots O_M$ distances. The topological properties at the $C_M \cdots C_B$ BCP [$\rho(r) = 0.06$ au.; $\nabla^2\rho_{(r)} = 0.03$ au.; $H_{(r)} < 0$] and $C_M \cdots O_M$ BCP [$\rho(r) = 0.04$ au.; $\nabla^2\rho(r) = 0.12$ au.; $H_{(r)} < 0$] are indicative of closed shell interactions (weak electrostatic or ionic bond) with a covalent character. The $C_M \cdots C_B$ interaction is

stronger than similar C···C interaction found at the TS of ethylene dimerization reaction over a model of acidic zeolite.[15]

The strongest interactions related to the confinement effects on the formed water molecule are O_M-$H_Z\cdots O_{Z1}$ and O_M-$H\cdots O_Z$. The electron density properties at the BCP indicate that they are HB interactions, their $\rho(r)$ values are higher than the other confinement interactions, showing the importance of water molecule in stabilizing the carbenium ion.

In addition, we found 10 C_B-$H\cdots O_Z$ interactions in H-ZSM-5 and 13 in H-Beta; 3 $O_Z\cdots\pi CC$ in H-ZSM-5 (and none in H-Beta); 3 C_M-$H\cdots O_Z$ in H-ZSM-5 and 2 in H-Beta, and finally one $C_M\cdots O_Z$. The latter are related to the confinement on the benzene molecule and also to the formed methyl cation. Additionally, $H\cdots O_Z$ interactions are shown involving one hydrogen atom from the organic molecule and two (or more) oxygen atoms from the zeolite (See Figures 3c-4c). From the electron density properties at the BCPs, the observed ranges show that all interactions correspond to closed shell interactions, only the interactions related to confinement of water show covalent character [$H(r) < 0$]. In order to give a better comprehension of the adsorbate-catalyst interactions, Figure S3 of supporting informations shows a simple scheme of the cavity and interactions found with QTAIM methodology for TS in H-ZSM-5.

The bond breaking and bond forming processes represent 72.5 % of total density in H-ZSM-5 and 74.1 % in H-Beta, while 27.7 % and 25.9 % correspond to the confinement effect, in H-ZSM-5 and H-Beta, respectively. The difference is related to the confinement effect on the methyl cation, where 4.9 % is in H-ZSM-5 and 3.3 % in H-Beta. No significant differences are observed on the confinement of benzene and water molecules, in accordance with the previous idea of the key role played by the oxygen atoms of the zeolite framework on the stability of the carbocation.[13-14] The major activation energy observed in H-ZSM-5 is due to the fact that the energy is required not only for the bond forming/bond breaking, but also to guarantee the proper orientation of benzene molecule, the methyl cation and water, in order to allow the interaction that will give rise to the new C–C bond. Due to the smaller available space in H-ZSM-5, the energy involved in the TS formation is higher in H-ZSM-5 than in H-Beta.

In summary, in both TS the methyl cation is multi-coordinated, the following $H_2O\cdots CH_3^+\cdots C_B$ concerted bonds are formed. For this step, the stability of the TS is achieved owing to the stabilizing effect of the surrounding zeolite framework on the carbocationic species (CH_3^+) which is higher in H-ZSM-5 than H-Beta. Our results suggest the importance of the intermolecular interactions between the organic molecules and the walls of the zeolite in stabilizing the transition state. So, these interactions play a key role in stabilizing the positive charge of the carbocationic fragment, which is also interacting with water and benzene molecules.

***Intermediate*:**

In the next step of the reaction, the key interactions are C_M–C_B bond formed; the guest-guest interactions (between the intermediate and water molecule) and the interactions related to the confinement effects (Table 5). The total electron density considered achieves 0.4429 u.a. and 0.3903 u.a. for H-ZSM-5 and H-Beta, respectively.

The formation of C_M–C_B bond gives rise to the intermediate, then the major contribution to the stabilization energy should be the one involved in forming this bond. In turn, the intermediate is stabilized by host-guest interactions with the catalyst and guest-guest interactions with the water molecule formed in the previous step. It can be observed that water contributes to stabilizing the charge of the carbocationic intermediate, in which the charge is distributed throughout the molecule (the sum of net atomic charge Σq (Ω) in intermediate fragment is + 0.98 *e* in both zeolites). By focusing on the confinement effect, we can refer the analysis to the effect on the water molecule and discriminate it from the confinement effect on the intermediate itself.

This intermediate is stabilized by different types of non-covalent interactions as C–H$\cdots$$O_Z$ [where ρ(r) values range from 0.0145 au. to 0.001 au.; and $\nabla^2\rho$(r) and H(r) values are positive] and C$\cdots$$O_Z$ with oxygen atoms of the zeolite [where ρ(r) values range from 0.013 au. to 0.0026 au.]. Only in H-Beta the basic and acid oxygen atoms of the catalyst are involved in these stabilizing interactions.

The intermediate was found to be destabilized (regarding to the co-adsorbed complex) in both zeolites. That is, the reaction energies (E_{rxn}) show that the intermediate is less stable than the co-adsorbed complex by about 60 kcal mol^{-1} in both zeolites. Comparing the

energies related to the TS, the stabilization is higher in H-ZSM-5 (18.4 kcal mol^{-1}) than in H-Beta (14.4 kcal mol^{-1}).

In principle, one can observe that the sum of the electron density at the BCP is higher in H-ZSM-5 than in H-Beta. The contribution of total electron density to the guest-guest interactions (6.8 % in H-ZSM-5 vs 6.8 % in H-Beta), and the contribution to the confinement on water molecule (10.6 % in H-ZSM-5 vs 11.8 % in H-Beta) shows similar values in both zeolites. However, the contribution related to the newly formed bond is higher in H-Beta than H-ZSM-5 (58.7% vs 51.8%). In turn, higher confinement or stabilization of intermediate is observed on the zeolite of smaller cavity (30.8 % in H-ZSM-5 vs 22.7% in H-Beta) as we expected.

These results suggest the importance of confinement effect in the stabilization of carbocationic intermediate. Energy stabilization in H-ZSM-5 is higher than in H-Beta, and higher quantity and contribution of the interactions with the oxygen of the cavity are observed (20 interactions in H-ZSM5 vs 17 in H-Beta), indicating such interactions involved in the stabilization of this intermediate are important.

4. Conclusions

In the present work we study the adsorbate-catalyst interactions between confined molecules and zeolites, and their relationship with energies involved in the reaction of methylation of benzene by methanol in H-ZSM-5 and H-Beta zeolites. The Quantum Theory of Atoms in Molecules was applied in order to gain a deeper understanding of electronic features that take place in the cavity of the catalyst and their role in the confinement effect.

The topological analysis of species involved in the reaction showed the presence of several interactions among organic molecules, as well as between the organic molecules and the oxygen atoms of the zeolitic fragment. Through the analysis of the electron density distribution we discriminated between interactions related to confinement effect and the reaction itself (adsorption, co-adsorption, bond breaking and bond forming processes). Our results show that the electron density analysis of host-guest interactions between organic species and two zeolite catalysts with different topologies provide valuable information

about the confinement effect and its relationship with the energetic parameters of the reaction.

In methanol adsorption, the main O_{Z1}-$H_Z\cdots O_M$ interaction related with the adsorption process on the zeolite acid site represents 75 % of total density contribution in H-ZSM-5 and 80.5 % in H-Beta. And weak interactions related to the confinement effect signifies 13.7 % in H-ZSM-5 and 12.2 % in H-Beta, demonstrating the effect of the size of the cavity in relation to the confinement effect and the adsorption energy. This is reflected in a greater stabilization of confined species within the cavity of H-ZSM-5.

In the co-adsorption process, the strength of the interactions related to adsorption and co-adsorption process is higher in the catalyst with larger cavity. However, the confinement effects are higher in the smaller zeolite, explaining from an electronic viewpoint the reason why the stabilization energy is higher in H-ZSM-5 than H-Beta. In this step, the stabilization is dominated by the confinement effect of the catalyst on the reactant species.

In TS the methyl cation is multi-coordinated, the following $H_2O\cdots CH_3^+\cdots C_B$ concerted bonds are formed. For this step, in both catalysts the properties of interactions related to bond forming and bond breaking are similar and, insignificant differences on the confinement of benzene and water molecules are observed. Thus, the stability of the TS is achieved due to the stabilizing effect of the surrounding zeolite framework on the carbocationic species (CH_3^+) which is higher in H-ZSM-5 than in H-Beta. However, the energy involved in the TS formation is smaller in H-Beta than in H-ZSM-5 due to the higher available space in the largest cavity that guarantees the proper orientation of benzene, methyl cation and water, in order to allow the interaction that will give rise to the new C–C bond.

In the intermediate, the major contribution to the stabilization energy is related to the newly formed C_M–C_B bond, and is higher in H-Beta than in H-ZSM-5. In turn, the intermediate is stabilized by guest-guest interactions with the water molecule formed in the previous step and host-guest interactions with the catalyst. The last ones related with the confinement effect show higher confinement or stabilization of intermediate on the zeolite of smaller cavity.

Summing up, our results showed that the analysis of electron density distribution could be used for providing new insights for the understanding of confinement effects inside zeolite cavities

Supporting Information

Supporting Information may be found in the online version of this article.

Acknowledgements

The authors acknowledge to Agencia Nacional de Promoción Científica y Tecnológica (grant FONCYT-PICT-0465), Secretaría de Ciencia y Tecnología de la Universidad Nacional del Nordeste (SECYT-UNNE), and Consejo Nacional de Investigaciones Científicas y Técnicas (CONICET) of Argentina for financial support. The authors also acknowledge the use of CPUs from the High Performance Computing Center of the Northeastern of Argentina (CECONEA)

References

1. Corma, A., State of the Art and Future Challenges of Zeolites as Catalysts. *J. Catal.* **2003**, *216*, 298-312.

2. Derouane, E. G., Zeolites as Solid Solvents. *J. Mol. Catal. A: Chem.* **1998**, *134*, 29-45.

3. Gounder, R.; Iglesia, E., The Catalytic Diversity of Zeolites: Confinement and Solvation Effects within Voids of Molecular Dimensions *Chem. Commun.* **2013**, *49*, 3491-3509.

4. Bhan, A.; Iglesia, E., A Link between Reactivity and Local Structure in Acid Catalysis on Zeolites. *Acc. Chem. Res.* **2008**, *41*, 559-567.

5. Gounder, R.; Iglesia, E., The Roles of Entropy and Enthalpy in Stabilizing Ion-Pairs at Transition States in Zeolite Acid Catalysis. *Acc. Chem. Res.* **2012**, *45*, 229-238.

6. Li, X.; Sun, Q.; Li, Y.; Wang, N.; Lu, J.; Yu, J., Confinement Effect of Zeolite Cavities on Methanol-to-Olefin Conversion: A Density Functional Theory Study. *J. Phys. Chem. C* **2014**, *118*, 24935–24940.

7. Mazar, M. N.; Al-Hashimi, S.; Bhan, A.; Cococcioni, M., Methylation of Ethene by Surface Methoxides: A Periodic PBE+D Study across Zeolites. *The Journal of Physical Chemistry C* **2012**, *116*, 19385-19395.

8. De Moor, B. A.; Reyniers, M.-F.; Gobin, O. C.; Lercher, J. A.; Marin, G. B., Adsorption of C2−C8 n-Alkanes in Zeolites. *J. Phys. Chem. C* **2011**, *115*, 1204-1219.

9. Sacchetto, V.; Bisio, C.; Olivas Olivera, D. F.; Paul, G.; Gatti, G.; Braschi, I.; Berlier, G.; Cossi, M.; Marchese, L., Interactions of Toluene and n-Hexane on High Silica Zeolites: An Experimental and Computational Model Study. *J. Phys. Chem. C* **2015**, *119*, 24875-24886.

10. Resasco, D. E.; Wang, B.; Crossley, S., Zeolite-Catalysed C-C Bond Forming Reactions for Biomass Conversion to Fuels and Chemicals. *Catal. Sci. Technol.* **2016**, *6*, 2543-2559.

11. Sastre, G., Confinement Effects in Methanol to Olefins Catalysed by Zeolites: A Computational Review. *Front. Chem. Sci. Eng.* **2016**, *10*, 76-89.

12. Shen, W., A Theoretical Study of Confinement Effect of Zeolite on the Ethylene Dimerization Reaction. *Microporous Mesoporous Mater.* **2017**, *247*, 136-144.

13. Zalazar, M. F.; Peruchena, N. M., Topological Analysis of the Electronic Charge Density in the Ethene Protonation Reaction Catalyzed by Acidic Zeolite. *J. Phys. Chem. A* **2007**, *111*, 7848–7859.

14. Zalazar, M. F.; Peruchena, N. M., Topological Description of the Bond Breaking and Bond Forming Processes of the Alkene Protonation Reaction in the Zeolite Chemistry: An Aim Study. *J. Mol. Model.* **2011**, *17*, 2501-2511.

15. Zalazar, M. F.; Peruchena, N., Laplacian of the Electron Density: A Hole-Lump Interaction as a Tool to Study Stereoelectronic Control of Chemical Reactions. *J. Phys. Org. Chem.* **2014**, *27*, 327-335.

16. Zalazar, M. F.; Duarte, D. J. R.; Peruchena, N. M., Adsorption of Alkenes on Acidic Zeolites. Theoretical Study Based on the Electron Charge Density. *J. Phys. Chem. A* **2009**, *113*, 13797–13807.

17. Bader, R. F. W., *Atoms in Molecules. A Quantum Theory*; Oxford Science Publications, Clarendon Press: London, 1990.

18. Popelier, P. L. A., *Atoms in Molecules. An Introduction*; Pearson Education: Harlow, U.K., 2000.

19. Matta, C. F.; Boyd, R. J., *The Quantum Theory of Atoms in Molecules: From Solid State to DNA and Drug Design*; Wiley-VCH: Weinheim, 2007.

20. Van der Mynsbrugge, J.; Visur, M.; Olsbye, U.; Beato, P.; Bjørgen, M.; Van Speybroeck, V.; Svelle, S., Methylation of Benzene by Methanol: Single-Site Kinetics over H-ZSM-5 and H-Beta Zeolite Catalysts. *J. Catal.* **2012**, *292*, 201-212.

21. Lesthaeghe, D.; De Sterck, B.; Van Speybroeck, V.; Marin, G. B.; Waroquier, M., Zeolite Shape-Selectivity in the Gem-Methylation of Aromatic Hydrocarbons. *Angew. Chem. Int. Ed.* **2007**, *46*, 1311-1314.

22. Fang, H.; Zheng, A.; Xu, J.; Li, S.; Chu, Y.; Chen, L.; Deng, F., Theoretical Investigation of the Effects of the Zeolite Framework on the Stability of Carbenium Ions. *J. Phys. Chem. C* **2011**, *115*, 7429-7439.

23. Patet, R. E.; Caratzoulas, S.; Vlachos, D. G., Adsorption in Zeolites Using Mechanically Embedded ONIOM Clusters. *Phys. Chem. Chem. Phys.* **2016**, *18*, 26094-26106.

24. Gomes, G. J.; Zalazar, M. F.; Lindino, C. A.; Scremin, F. R.; Bittencourt, P. R. S.; Costa, M. B.; Peruchena, N. M., Adsorption of Acetic Acid and Methanol on H-Beta Zeolite: An Experimental and Theoretical Study. *Microporous Mesoporous Mater.* **2017**, *252*, 17-28.

25. Zhao, Y.; Truhlar, D. G., The Minnesota Density Functionals and Their Applications to Problems in Mineralogy and Geochemistry. *Rev. Mineral. Geochem.* **2010**, *71*, 19-37.

26. Zhao, Y.; Truhlar, D. G., Benchmark Data for Interactions in Zeolite Model Complexes and Their Use for Assessment and Validation of Electronic Structure Methods. *J. Phys. Chem. C* **2008**, *112*, 6860-6868.

27. Maihom, T.; Boekfa, B.; Sirijaraensre, J.; Nanok, T.; Probst, M.; Limtrakul, J., Reaction Mechanisms of the Methylation of Ethene with Methanol and Dimethyl Ether over H-ZSM-5: An ONIOM Study. *J. Phys. Chem. C* **2009**, *113*, 6654–6662.

28. Kongpatpanich, K.; Nanok, T.; Boekfa, B.; Probst, M.; Limtrakul, J., Structures and Reaction Mechanisms of Glycerol Dehydration over H-ZSM-5 Zeolite: A Density Functional Theory Study. *Phys. Chem. Chem. Phys.* **2011**, *13*, 6462-6470.

29. Maihom, T.; Pantu, P.; Tachakritikul, C.; Probst, M.; Limtrakul, J., Effect of the Zeolite Nanocavity on the Reaction Mechanism of n-Hexane Cracking: A Density Functional Theory Study. *J. Phys. Chem. C* **2010**, *114*, 7850-7856.

30. Charoenwiangnuea, P.; Maihom, T.; Kongpracha, P.; Sirijaraensre, J.; Limtrakul, J., Adsorption and Decarbonylation of Furfural over H-ZSM-5 Zeolite: A DFT Study. *RSC Advances* **2016**, *6*, 105888-105894.

31. Gomes, J.; Zimmerman, P. M.; Head-Gordon, M.; Bell, A. T., Accurate Prediction of Hydrocarbon Interactions with Zeolites Utilizing Improved Exchange-Correlation Functionals and QM/MM Methods: Benchmark Calculations of Adsorption Enthalpies and Application to Ethene Methylation by Methanol. *J. Phys. Chem. C* **2012**, *116*, 15406-15414.

32. Frisch, M. J., et al. *Gaussian 09*, revision A.01; Gaussian, Inc.: Wallingford, CT, 2009.

33. Keith, T. A. *Aimall* (Version 13.05.06); TK Gristmill Software: Overland Park KS, USA, 2013.

34. Wen, Z.; Yang, D.; He, X.; Li, Y.; Zhu, X., Methylation of Benzene with Methanol over HZSM-11 and HZSM-5: A Density Functional Theory Study. *J. Mol. Catal. A: Chem.* **2016**, *424*, 351-357.

35. Saepurahman; Visur, M.; Olsbye, U.; Bjørgen, M.; Svelle, S., In Situ FT-IR Mechanistic Investigations of the Zeolite Catalyzed Methylation of Benzene with Methanol: H-ZSM-5 Versus H-Beta. *Top. Catal.* **2011**, *54*, 1293–1301.

36. Svelle, S.; Visur, M.; Olsbye, U.; Saepurahman; Bjørgen, M., Mechanistic Aspects of the Zeolite Catalyzed Methylation of Alkenes and Aromatics with Methanol: A Review. *Top. Catal.* **2011**, *54*, 897-906.

37. Lee, C. C.; Gorte, R. J.; Farneth, W. E., Calorimetric Study of Alcohol and Nitrile Adsorption Complexes in H-ZSM-5. *J. Phys. Chem. B* **1997**, *101*, 3811-3817.

38. Arstad, B.; Nicholas, J. B.; Haw, J. F., Theoretical Study of the Methylbenzene Side-Chain Hydrocarbon Pool Mechanism in Methanol to Olefin Catalysis. *J. Am. Chem. Soc.* **2004**, *126*, 2991-3001.

39. Politzer, P.; Murray, J. S., A Unified View of Halogen Bonding, Hydrogen Bonding and Other σ-Hole Interactions In *Noncovalent Forces. Challenges and Advances in Computational Chemistry and Physics*, Scheiner, S., Ed. Springer International Publishing Cham, Switzerland, 2015; Vol. 19, pp 291–322.

40. Chamorro, E. R.; Sequeira, A. F.; Zalazar, M. F.; Peruchena, N. M., Theoretical Analysis of the Electronic Properties of the Sex Pheromone and Its Analogue Derivatives in the Female Processionary Moth Thaumetopoea Pytiocampa. *Bioorg. Med. Chem.* **2008**, *16*, 8535-45.

41. Bader, R. F. W., A Bond Path: A Universal Indicator of Bonded Interactions. *J. Phys. Chem. A* **1998**, *102*, 7314-7323.

42. Arnold, W. D.; Oldfield, E., The Chemical Nature of Hydrogen Bonding in Proteins Via NMR: J-Couplings, Chemical Shifts, and AIM Theory. *J. Am. Chem. Soc.* **2000**, *122*, 12835-12841.

43. Cremer, D.; Kraka, E., A Description of the Chemical Bond in Terms of Local Properties of the Electron Density and Energy. *Croat. Chem. Acta* **1984**, *57*, 1259–1281.

44. Jenkins, S.; Morrison, I., The Chemical Character of the Intermolecular Bonds of Seven Phases of Ice as Revealed by Ab Initio Calculation of Electron Densities. *Chem. Phys. Lett.* **2000**, *317*, 97-102.

45. Svelle, S.; Tuma, C.; Rozanska, X.; Kerber, T.; Sauer, J., Quantum Chemical Modeling of Zeolite-Catalyzed Methylation Reactions: Toward Chemical Accuracy for Barriers. *J. Am. Chem. Soc.* **2009**, *131*, 816-825.

46. Nguyen, C. M.; Reyniers, M.-F.; Marin, G. B., Theoretical Study of the Adsorption of C1-C4 Primary Alcohols in H-ZSM-5. *Phys. Chem. Chem. Phys.* **2010**, *12*, 9481-9493.

47. Van der Mynsbrugge, J.; Hemelsoet, K.; Vandichel, M.; Waroquier, M.; Van Speybroeck, V., Efficient Approach for the Computational Study of Alcohol and Nitrile Adsorption in H-ZSM-5. *J. Phys. Chem. C* **2012**, *116*, 5499-5508.

48. Stückenschneider, K.; Merz, J.; Schembecker, G., Molecular Interactions of Alcohols with Zeolite BEA and MOR Frameworks. *J. Mol. Model.* **2013**, *19*, 5611-5624.

49. Zecchina, A.; Bordiga, S.; Spoto, G.; Scarano, D.; Spano, G.; Geobaldo, F., Ir Spectroscopy of Neutral and Ionic Hydrogen-Bonded Complexes Formed Upon Interaction of CH_3OH, C_2H_5OH, $(CH_3)_2O$, $(C_2H_5)_2O$ and C_4H_8O with H-Y, H-ZSM-5 and H-Mordenite: Comparison with Analogous Adducts Formed on the H-Nafion Superacidic Membrane. *J. Chem. Soc., Faraday Trans.* **1996**, *92*, 4863-4875.

50. Kotrla, J.; Nachtigallová, D.; Kubelková, L.; Heeribout, L.; Doremieux-Morin, C.; Fraissard, J., Hydrogen Bonding of Methanol with Bridged OH Groups of Zeolites: Ab Initio Calculation, 1H NMR and FTIR Studies. *J. Phys. Chem. B* **1998**, *102*, 2454-2463.

51. Mirth, G.; Lercher, J. A.; Anderson, M. W.; Klinowski, J., Adsorption Complexes of Methanol on Zeolite ZSM-5 *J. Chem. Soc., Faraday Trans.* **1990**, *86*, 3039-3044.

52. Pazé, C.; Bordiga, S.; Lamberti, C.; Salvalaggio, M.; Zecchina, A.; Bellussi, G., Acidic Properties of H−B Zeolite as Probed by Bases with Proton Affinity in the 118−204 Kcal Mol^{-1} Range: A FTIR Investigation. *J. Phys. Chem. B* **1997**, *101*, 4740-4751.

53. Haase, F.; Sauer, J., Interaction of Methanol with Brönsted Acid Sites of Zeolite Catalysts: An Ab Initio Study. *J. Am. Chem. Soc.* **1995**, *117*, 3780-3789.

54. Grabowski, S. J., What Is the Covalency of Hydrogen Bonding? *Chem. Rev.* **2011**, *111*, 2597-2625.

Figure captions

Figure 1. (a) Adsorbed methanol, (b) co-adsorbed benzene onto methanol complex, (c) TS for methylation of benzene by methanol and (d) intermediate, in H-ZSM-5 and H-Beta zeolites.

Figure 2. Molecular electrostatic potential on the 0.001 au. electron density isosurface for H-ZSM-5 and H-Beta zeolite. The red and blue colors indicate negative and positive regions, respectively, varying between – 32.81 kcal mol^{-1} and + 61.80 kcal mol^{-1}. The molecular graphs of ρ(r) is also observed.

Figure 3. Molecular graphs for: (a) adsorbed methanol, (b) co-adsorbed benzene onto methanol complex, (c) TS for methylation of benzene by methanol and (d) intermediate in H-ZSM-5 zeolite. Big circles correspond to attractors attributed to nuclei, lines connecting the nuclei are the bond paths and the small red circles on them are the bond critical points (BCP). Terminal H atoms of Si-H bonds in the zeolite; ring and cage critical points were omitted for clarity.

Figure 4. Molecular graphs for: (a) adsorbed methanol, (b) co-adsorbed benzene onto methanol complex, (c) TS for methylation of benzene by methanol and (d) intermediate in H-Beta zeolite. Big circles correspond to attractors attributed to nuclei, lines connecting the nuclei are the bond paths and the small red circles on them are the bond critical points (BCP). Terminal H atoms of Si-H bonds in the zeolite; ring and cage critical points were omitted for clarity.

Table 1. Adsorption and coadsorption energies (E_{ads} and E_{coads}), energies corrected by ZPE ($E_{ads+zpe}$ and $E_{coads+zpe}$), adsorption enthalpies ($\Delta H°$), activation energies (E_a), activation enthalpies ($\Delta H^{\neq}°$), and reaction energies (E_{rxn}) in (kcal mol^{-1}).

	Methanol [a)]			**Co-adsorbed Benzene**			**TS**			**Intermediate**		
	E_{ads}	$E_{ads+zpe}$	$\Delta H°_{(298K)}$	E_{coads}	$E_{coads+zpe}$	$\Delta H°_{(298K)}$	E_a	E_{a+zpe}	$\Delta H^{\neq}°_{(298K)}$	E_{rxn}	$E_{rxn+zpe}$	$\Delta H_{rxn}°_{(298K)}$
H-ZSM-5												
B3LYP/6-31G(d)	-28.11	-27.16	-27.33	-3.8	-3.48	-2.86	36.05	35.91	35.78	18.96	18.87	18.99
M06-2X/6-31G(d)	-32.71	-32.21	-32.42	-17.45	-17.75	-17.20	40.34	40.85	40.70	21.95	22.24	22.34
SP M06-2X/6-31++G(d,p)[b)]	-31.84	-31.35	-31.55	-19.38	-19.68	-19.38	40.73	41.27	41.14	22.07	22.36	22.46
H-Beta												
B3LYP/6-31G(d)	-25.07	-24.48	-24.61	-3.33	-2.65	-1.94	32.01	32.11	31.71	16.39	20.72	20.77
M06-2X/6-31G(d)	-28.98	-28.75	-29.00	-14.88	-13.85	-13.54	36.88	37.10	36.98	22.50	21.97	22.44
SP M06-2X/6-31++G(d,p) [b)]	-27.57	-27.34	-27.59	-16.70	-15.36	-15.67	37.24	37.49	37.37	21.32	20.79	21.26

[a] Experimental value of -27.5 kcal mol^{-1} for methanol adsorption on H-ZSM-5 from reference 37.

[b] The SP calculations were approximated to 298 K, by using the ZPE and thermal corrections of the lower level M06-2X/6-31G(d) calculations.

Table 2: Bond Distance (Å) and Local Topological Properties (au.) of the Electronic Charge Density Distribution Calculated at the Position of the Bond Critical Points for Adsorbed methanol in H-ZSM-5 and H-Beta zeolites. [a, b)]

	Interaction	$d_{X\cdots Y}$	$\rho(\mathbf{r})$	$\nabla^2\rho(\mathbf{r})$	$H(\mathbf{r})$
H-ZSM-5					
Adsorption	O_{Z1}-$H_Z\cdots O_M$	1.36	0.1100	0.0148	–0.0690
	O_M-H$\cdots O_{Z2}$	2.24	0.0167	0.0600	0.0004
Confinement	O_M-H$\cdots O_Z$	2.26	0.0128	0.0426	0.0001
	C_M-H$\cdots O_Z$	2.94	0.0038	0.0153	0.0009
	C_M-H$\cdots O_Z$	2.97	0.0034	0.0139	0.0008
H-Beta					
Adsorption	O_{Z1}-$H_Z\cdots O_M$	1.27	0.1423	–0.2090	–0.1359
	O_M-H$\cdots O_{Z2}$	2.14	0.0196	0.0679	–0.0001
Confinement	O_M-H$\cdots O_Z$	2.42	0.0084	0.0328	0.0008
	C_M-H$\cdots O_Z$	2.90	0.0042	0.0172	0.0009
	C_M-H$\cdots O_Z$	3.14	0.0021	0.0097	0.0007
	C_M-H$\cdots O_Z$	4.18	0.0002	0.0009	0.0001

[a)] The electron density [ρ(r)], the Laplacian of electron density [$\nabla^2\rho$(r)], and the total energy density, [$H_{(r)}$] in au.

[b)] To identify the atoms and interactions, see the text and Figures 3 and 4

Table 3: Bond Distance (Å) and Local Topological Properties (au) of the Electronic Charge Density Distribution Calculated at the Position of the Bond Critical Points for Co-adsorbed Benzene onto Methanol Complex in H-ZSM-5 and H-Beta Zeolites. [a, b)]

	Interaction	$d_{X\cdots Y}$	$\rho(\mathbf{r})$	$\nabla^2\rho(\mathbf{r})$	$H(\mathbf{r})$
H-ZSM-5					
Adsorption (methanol)	O_{Z1}-$H_Z\cdots O_M$	1.16	0.1875	–0.5847	–0.2303
Co-adsorption (benzene)	C_M-H$\cdots C_B$	2.64	0.0089	0.0286	0.0011
Confinement (benzene)	C_B-H$\cdots O_Z$	2.48	0.0106	0.0384	0.0010
	C_B-H$\cdots O_Z$	2.56	0.0087	0.0315	0.0009
	C_B–H$\cdots O_Z$	2.58	0.0086	0.0319	0.0011
	C_B–H$\cdots O_Z$	2.67	0.0072	0.0271	0.0010
	C_B–H$\cdots O_Z$	2.69	0.0060	0.0224	0.0008
	C_B–H$\cdots O_Z$	2.73	0.0055	0.0209	0.0008
	C_B–H$\cdots O_Z$	2.78	0.0067	0.0244	0.0010
	C_B–H$\cdots O_Z$	2.78	0.0067	0.0244	0.0010
	C_B–H$\cdots O_Z$	2.84	0.0059	0.0216	0.0010
	C_B–H$\cdots O_Z$	2.90	0.0055	0.0188	0.0009
	C_B–H$\cdots O_Z$	2.91	0.0054	0.0203	0.0010
	$O_Z\cdots\pi$CC	3.20	0.0070	0.0221	0.0007
	$O_Z\cdots\pi$CC	3.32	0.0057	0.0184	0.0007
	$O_Z\cdots\pi$CC	3.41	0.0049	0.0159	0.0007
	$O_Z\cdots\pi$CC	3.44	0.0047	0.0151	0.0006
	$O_Z\cdots\pi$CC	3.52	0.0042	0.0135	0.0006
Confinement (methanol)	C_M–H$\cdots O_Z$	2.84	0.0041	0.0172	0.0009
	C_M–H$\cdots O_Z$	3.41	0.0012	0.0053	0.0004
	C_M–H$\cdots O_Z$	3.58	0.0010	0.0044	0.0003
	C_M–H$\cdots O_Z$	3.62	0.0008	0.0035	0.0003
	O_M–H$\cdots O_Z$	2.17	0.0144	0.0436	0.0003
H–Beta					
Adsorption (methanol)	O_{Z1}–$H_Z\cdots O_M$	1.14	0.1999	–0.6762	–0.2536
Co–adsorption (benzene)	O_M–H$\cdots C_B$	2.24	0.0164	0.0444	0.0005
	C_M–H$\cdots C_B$	2.74	0.0084	0.0269	0.0013
Confinement (benzene)	C_B–H$\cdots O_Z$	2.46	0.0095	0.0319	0.0005
	C_B–H$\cdots O_Z$	2.49	0.0097	0.0342	0.0008
	C_B–H$\cdots O_Z$	2.75	0.0057	0.0229	0.0010
	C_B–H$\cdots O_Z$	2.76	0.0056	0.0221	0.0010
	C_B–H$\cdots O_Z$	2.86	0.0057	0.0214	0.0011
	C_B–H$\cdots O_Z$	2.95	0.0043	0.0162	0.0008

	C_B–H···O_Z	2.95	0.0045	0.0171	0.0009
	C_B–H···O_Z	3.35	0.0014	0.0063	0.0005
	O_Z···πCC	3.05	0.0095	0.0347	0.0013
	O_Z···πCC	3.25	0.0071	0.0215	0.0006
	O_Z···πCC	3.32	0.0056	0.0200	0.0008
	O_Z···πCC	3.64	0.0029	0.0115	0.0006
Confinement (methanol)	C_M–H···O_Z	2.53	0.0085	0.0300	0.0008
	C_M–H···O_Z	4.20	0.0002	0.0009	0.0001

[a)] The electron density [ρ(r)], the Laplacian of electron density [$\nabla^2\rho$(r)], the local potential energy density, [V(r)], the local kinetic energy density [G(r)], and the total energy density, [$H_{(r)}$] in au.

[b)] To identify the atoms and interactions, see the text and Figures 3 and 4

Table 4: Bond Distance (Å) and Local Topological Properties (au) of the Electronic Charge Density Distribution Calculated at the Position of the Bond Critical Points for Transition States of Methylation of Benzene by Methanol in H–ZSM–5 and H–Beta Zeolites. [a, b)]

	Interaction	$d_{X\cdots Y}$	$\rho(\mathbf{r})$	$\nabla^2\rho(\mathbf{r})$	$H(\mathbf{r})$
H–ZSM–5					
Bond forming	$C_M\cdots C_B$	2.08	0.0634	0.0382	–0.0179
Bond breaking	$C_M\cdots O_M$	2.17	0.0428	0.1289	–0.0020
Bond formed	$O_M–H_Z$	0.98	0.3421	–2.0714	–0.5827
Confinement (H_2O)	$O_M–H_Z\cdots O_{Z1}$	1.99	0.0231	0.0758	–0.0005
	$O_M–H\cdots O_Z$	2.11	0.0171	0.0516	–0.0005
	$O_M\cdots O_Z$	3.00	0.0107	0.0426	0.0011
Confinement (benzene)	$C_B–H\cdots O_Z$	2.34	0.0128	0.0420	0.0004
	$C_B–H\cdots O_Z$	2.50	0.0101	0.0359	0.0009
	$C_B–H\cdots O_Z$	2.57	0.0088	0.0320	0.0010
	$C_B–H\cdots O_Z$	2.59	0.0076	0.0271	0.0008
	$C_B–H\cdots O_Z$	2.72	0.0065	0.0254	0.0011
	$C_B–H\cdots O_Z$	2.75	0.0056	0.0215	0.0010
	$C_B–H\cdots O_Z$	2.79	0.0061	0.0233	0.0010
	$C_B–H\cdots O_Z$	2.84	0.0057	0.0213	0.0010
	$C_B–H\cdots O_Z$	2.88	0.0045	0.0184	0.0010
	$C_B–H\cdots O_Z$	3.13	0.0028	0.0112	0.0007
	$O_Z\cdots\pi CC$	3.00	0.0098	0.0345	0.0011
	$O_Z\cdots\pi CC$	3.15	0.0074	0.0249	0.0008
	$O_Z\cdots\pi CC$	3.60	0.0030	0.0108	0.0006
Confinement (methyl cation)	$C_M–H\cdots O_Z$	2.17	0.0195	0.0626	–0.0001
	$C_M–H\cdots O_Z$	2.59	0.0068	0.0254	0.0009
	$C_M–H\cdots O_Z$	3.02	0.0040	0.0155	0.0009
H–Beta					
Bond forming	$C_M\cdots C_B$	2.05	0.0678	0.0309	–0.0212
Bond breaking	$C_M\cdots O_M$	2.20	0.0406	0.1263	–0.0014
Bond formed	$O_M–H_Z$	0.98	0.3444	–2.0663	–0.5837
Confinement (H_2O)	$O_M–H\cdots O_{Z\,1}$	1.96	0.0237	0.0758	–0.0005
	$O_M–H\cdots O_Z$	2.12	0.0168	0.0513	–0.0005
	$O_M\cdots O_Z$	2.93	0.0118	0.0438	0.0008
Confinement (benzene)	$C_B–H\cdots O_Z$	2.37	0.0126	0.0418	0.0005
	$C_B–H\cdots O_Z$	2.49	0.0100	0.0357	0.0009

	C_B–H···O_Z	2.55	0.0084	0.0290	0.0007
	C_B–H···O_Z	2.58	0.0074	0.0268	0.0008
	C_B–H···O_Z	2.67	0.0076	0.0280	0.0011
	C_B–H···O_Z	2.69	0.0071	0.0272	0.0011
	C_B–H···O_Z	2.73	0.0075	0.0278	0.0012
	C_B–H···O_Z	2.75	0.0051	0.0199	0.0009
	C_B–H···O_Z	2.95	0.0036	0.0154	0.0009
	C_B–H···O_Z	3.21	0.0024	0.0099	0.0006
	C_B–H···O_Z	3.28	0.0017	0.0072	0.0005
	C_B–H···O_Z	3.29	0.0016	0.0070	0.0005
	C_B–H···O_Z	3.58	0.0011	0.0041	0.0003
Confinement (methyl cation)	C_M–H···O_Z	2.36	0.0118	0.0381	0.0002
	C_M–H···O_Z	2.52	0.0086	0.0311	0.0009
	C_M···O_Z	3.04	0.0100	0.0397	0.0014

[a] The electron density [ρ(r)], the Laplacian of electron density [$\nabla^2\rho$(r)], and the total energy density, [$H_{(r)}$] in au.

[b] To identify the atoms and interactions, see the text and Figures 3 and 4

Table 5: Bond Distance (Å) and Local Topological Properties (au) of the Electronic Charge Density Distribution Calculated at the Position of the Bond Critical Points for intermediate specie in H–ZSM–5 and H–Beta Zeolites. [a, b)]

	Interaction	$d_{X\cdots Y}$	$\rho(r)$	$\nabla^2\rho(\mathbf{r})$	$H(\mathbf{r})$
H–ZSM–5					
Bond formed	C_M–C_B	1.54	0.2293	–0.4903	–0.1800
Guest–guest	$C_B\cdots O_M$	2.62	0.0180	0.0581	0.0007
Guest–guest	C_M–$H\cdots O_M$	2.36	0.0122	0.0453	0.0011
Confinement (water)	O_M–$H_{Z1}\cdots O_{Z1}$	1.96	0.0238	0.0792	–0.0003
	O_M–$H\cdots O_Z$	2.15	0.0155	0.0476	–0.0004
	$O_M\cdots O_{Z2}$	3.19	0.0076	0.0297	0.0010
Confinement (intermediate)	$C_M\cdots O_Z$	3.04	0.0083	0.0334	0.0013
	$C_B\cdots O_Z$	3.12	0.0082	0.0282	0.0009
	$C_B\cdots O_Z$	3.21	0.0061	0.0224	0.0010
	$C_B\cdots O_Z$	3.72	0.0026	0.0091	0.0005
	C_B–$H\cdots O_Z$	2.28	0.0145	0.0507	0.0007
	C_B–$H\cdots O_Z$	2.41	0.0108	0.0375	0.0007
	C_B–$H\cdots O_Z$	2.51	0.0101	0.0377	0.0011
	C_B–$H\cdots O_Z$	2.57	0.0090	0.0341	0.0012
	C_B–$H\cdots O_{Z1}$	2.60	0.0083	0.0301	0.0009
	C_B–$H\cdots O_Z$	2.64	0.0084	0.0315	0.0012
	C_B–$H\cdots O_Z$	2.65	0.0071	0.0271	0.0011
	C_B–$H\cdots O_Z$	2.68	0.0063	0.0241	0.0009
	C_B–$H\cdots O_Z$	2.76	0.0049	0.0193	0.0009
	C_B–$H\cdots O_Z$	2.87	0.0051	0.0193	0.0010
	C_B–$H\cdots O_Z$	3.14	0.0024	0.0099	0.0007
	C_B–$H\cdots O_Z$	3.33	0.0016	0.0066	0.0005
	C_M–$H\cdots O_Z$	2.49	0.0100	0.0343	0.0008
	C_M–$H\cdots O_Z$	2.72	0.0071	0.0254	0.0011
	C_M–$H\cdots O_Z$	3.13	0.0033	0.0129	0.0007
	C_M–$H\cdots O_Z$	3.15	0.0023	0.0098	0.0007
H–Beta					
Bond formed	C_M–C_B	1.54	0.2292	–0.4894	–0.1800
Guest–guest	$C_B\cdots O_M$	2.92	0.0117	0.0397	0.0009
Guest–guest	C_M–$H\cdots O_M$	2.28	0.0148	0.0519	0.0008
Confinement (water)	O_M–$H_Z\ldots O_{Z1}$	1.93	0.0245	0.0785	–0.0002
	O_M–$H\cdots O_Z$	2.28	0.0117	0.0379	0.0001

	$O_M \cdots O_{Z2}$	3.03	0.0098	0.0360	0.0008
Confinement (intermediate)	$C_B \cdots O_{Z2}$	2.79	0.0132	0.0502	0.0016
	$C_B \cdots O_{Z1}$	3.05	0.0096	0.0326	0.0010
	C_B–H$\cdots O_Z$	2.46	0.0094	0.0313	0.0005
	C_B–H$\cdots O_Z$	2.61	0.0073	0.0263	0.0008
	C_B–H$\cdots O_Z$	2.64	0.0078	0.0301	0.0012
	C_B–H$\cdots O_Z$	2.75	0.0054	0.0203	0.0009
	C_B–H$\cdots O_Z$	2.77	0.0050	0.0193	0.0009
	C_B–H$\cdots O_Z$	2.80	0.0048	0.0194	0.0010
	C_B–H$\cdots O_Z$	2.83	0.0058	0.0227	0.0011
	C_B–H$\cdots O_Z$	2.94	0.0046	0.0180	0.0010
	C_B–H$\cdots O_Z$	3.19	0.0023	0.0096	0.0007
	C_B–H$\cdots O_Z$	3.44	0.0010	0.0047	0.0004
	C_B–H$\cdots O_Z$	3.50	0.0011	0.0047	0.0004
	C_M–H$\cdots O_Z$	2.73	0.0061	0.0218	0.0009
	C_M–H$\cdots O_Z$	3.02	0.0035	0.0139	0.0008
	C_M–H$\cdots O_Z$	3.50	0.0011	0.0047	0.0004
	C_M–H$\cdots O_Z$	3.75	0.0007	0.0029	0.0003

[a] The electron density [ρ(r)], the Laplacian of electron density [$\nabla^2\rho$(r)], and the total energy density, [$H_{(r)}$] in au.

[b] To identify the atoms and interactions, see the text and Figures 3 and 4

Figure 1.

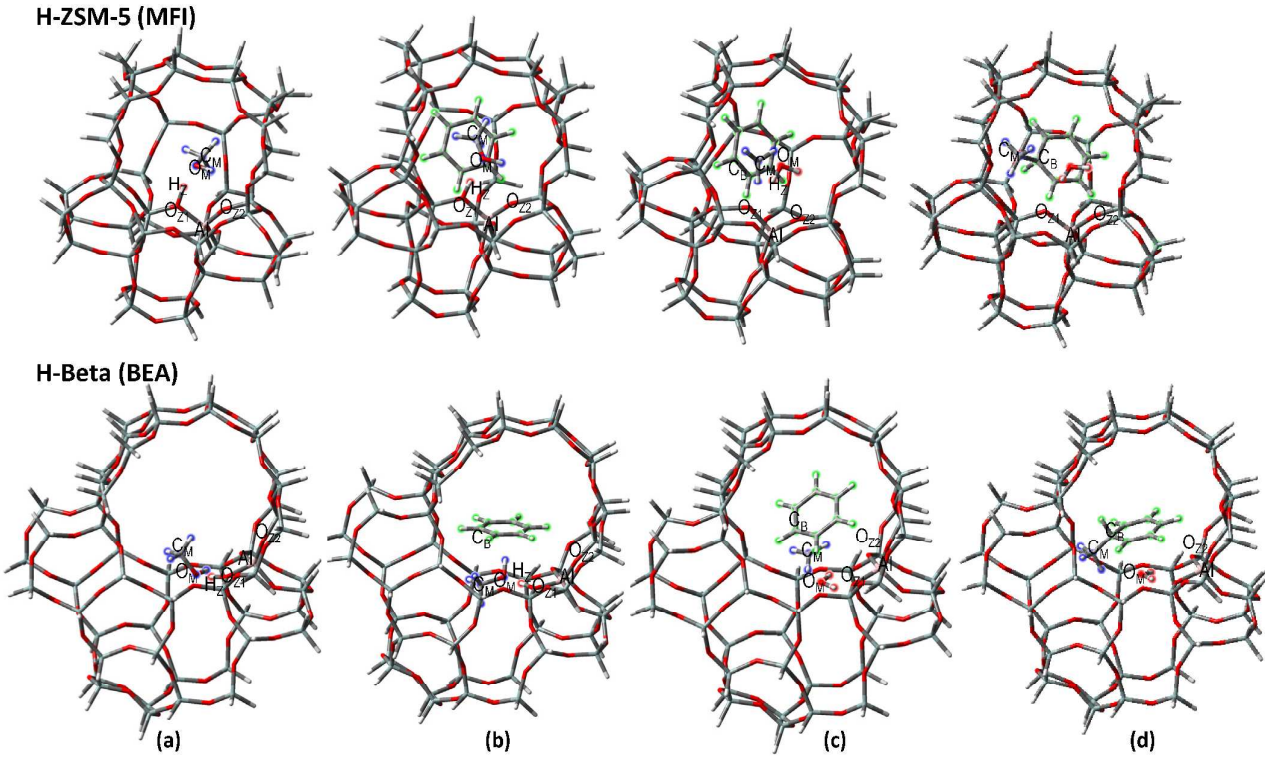

Figure 2.

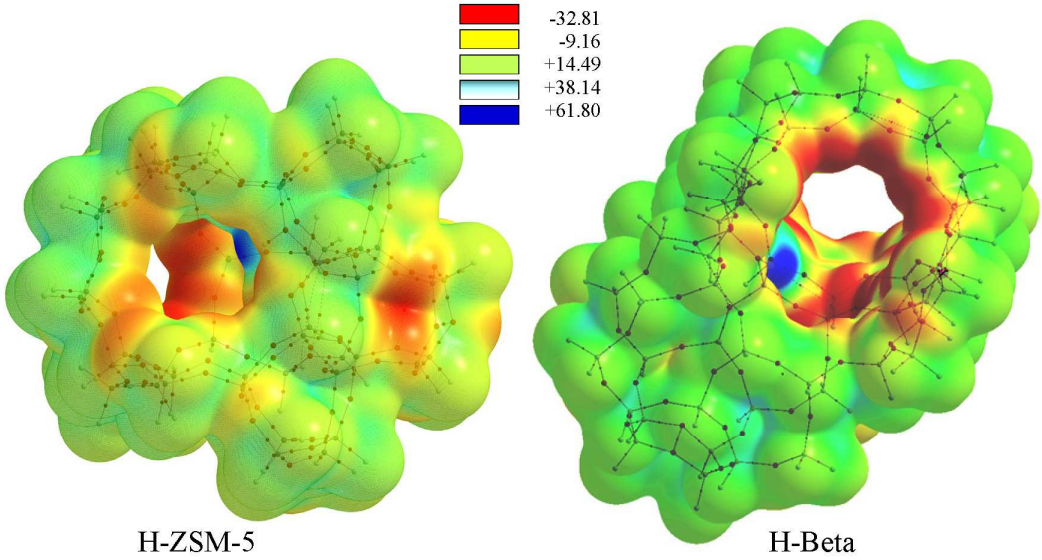

Figure 3.

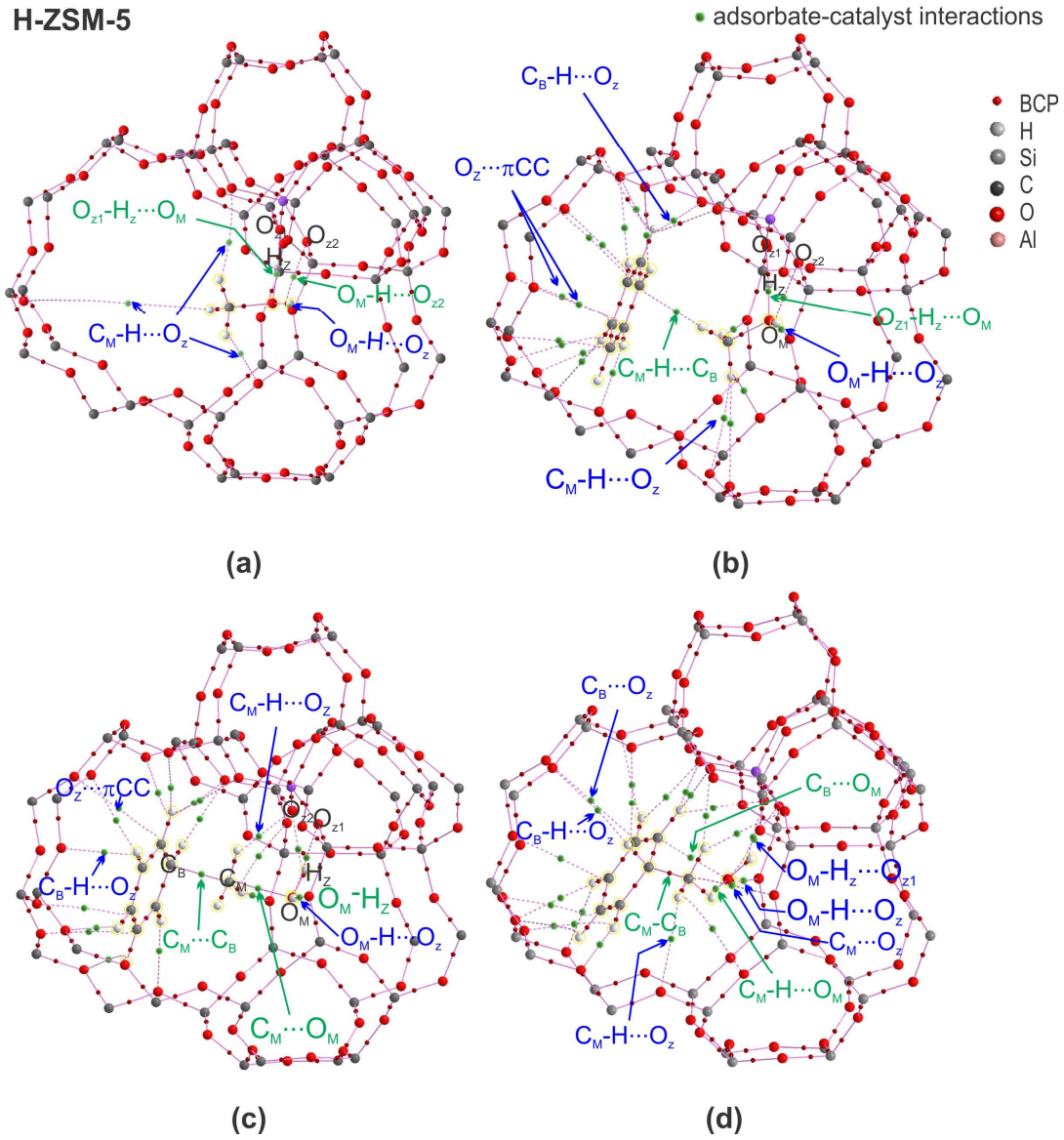

Figure 4.

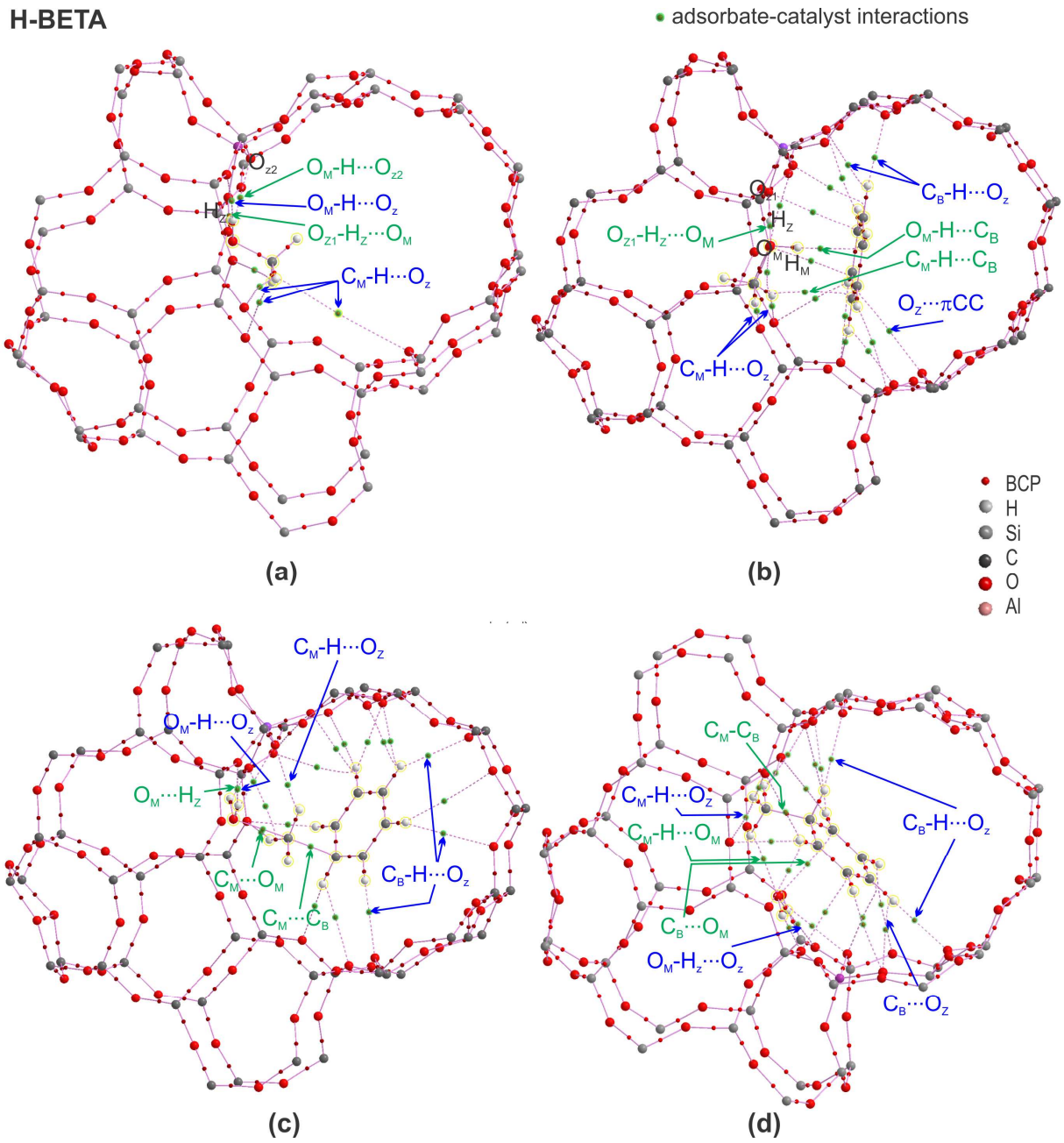
H-BETA
adsorbate-catalyst interactions
O_{z2}
O_M-H···O_{z2}
O_M-H···O_z
H_Z
O_{Z1}-H_Z···O_M
C_M-H···O_z
(a)
C_B-H···O_z
O_{Z1}
H_Z
O_{Z1}-H_Z···O_M
O_M-H···C_B
O_M
H_M
C_M-H···C_B
O_z···πCC
C_M-H···O_z
(b)
BCP
H
Si
C
O
Al
C_M-H···O_z
O_M-H···O_z
O_M···H_Z
C_M···O_M
C_M···C_B
C_B-H···O_z
(c)
C_M-C_B
C_M-H···O_z
C_M-H···O_M
C_B-H···O_z
C_B···O_M
O_M-H_z···O_z
C_B···O_z
(d)

Table of Contents Graphic (TOC)